Multiobjective Optimal Design of an Axial Flux Permanent Magnet Generator for Directly Coupled Wind Turbines

Narges Taran, Mohammad Ardebili

Abstract— Factors such as high efficiency, high power density, the possibility of realizing a compact multistage machine and the feasibility of applying a large number of poles make the Axial Flux Permanent Magnet (AFPM) generators highly appealing for use as low speed wind power generators. This study puts forth a multi-objective optimization of the efficiency and power density of a low speed AFPM synchronous generator. The optimization problem was formulated by means of general sizing equations and then Genetic Algorithm (GA) was utilized. This study uses a weighted fitness function which offers a tool for ascertaining the priority of objective functions. This fitness function includes two variables whereby an increase in either of them leads to more improvement in one of the objective functions than in the other. The merits of this method are especially palpable in situations where it is necessary to prioritize the objective functions as is indeed the case with generators used in wind turbines which should have not only a high efficiency but also a reduced weight and volume. Finally, the results are verified through the three dimensional Finite Element Method (3D-FEM).

Index Terms— Axial Flux Permanent Magnet (AFPM) machine, Genetic Algorithm (GA), Multi-objective optimization, Synchronous Generator, Three Dimensional Finite Element Method (3D-FEM).

1 INTRODUCTION

In recent years, Axial Flux Permanent Magnet (AFPM) synchronous machines have been growing in popularity and have received an increasing amount of attention in direct drive wind power application [1], [2], [3]. Eliminating the problematic gearbox in direct drive wind turbines decreases the rotation speed of the generator shaft. To offset the low speed, there is an inevitable need for a large number of poles and consequently a much increased diameter, both of which may be done more easily in axial flux machines than in conventional radial flux ones due to the disc-shape structure of AFPM machines. Other factors such as their high efficiency and high power density make the axial flux permanent magnet generators highly appealing for use as direct drive wind power generators [4].

AFPM generators are used in a variety of topologies and structures. For instance, they could be single-sided with only one stator and one rotor core, which poses the problem of balanced airgap preservation [5]. To solve this problem, the double-sided structure is used which contains two stator cores and one internal rotor core, known as Axial Flux Internal Rotor (AFIR), or two rotor cores and one internal stator core, known as the TORUS structure. The ultimate goal of this study is to design a low speed (100 rpm) generator with 1 kW output power. It has been proved that in low power applications the TORUS structure yields a higher power density [6]. The stator core could be slotted or slotless while the slotted stator results in a lower airgap and magnet thickness and also a higher mechanical strength in the winding configuration [7]. The rotor core could have surface mounted Permanent Magnet (PM)s or embedded PMs. Given the centrifugal force, embedded PMs are a better choice whereas considering the low speed in direct drive applications as well as the need for placing a high number of PMs makes it more practical to use surface mounted PMs. Fig. 1 illustrates an AFPM generator with the TORUS-S (double rotor and slotted stator) structure and surface mounted PMs.

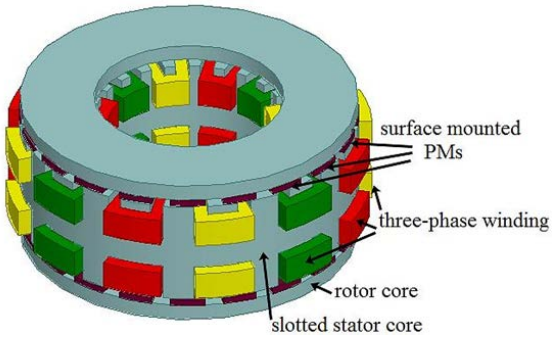

Fig. 1. TORUS-S generator

Regarding the construction of AFPM machines, different cross sections in different axial lengths will lead to different views. Considering radial cross sections will not solve the problem because the flux density varies with different diameters. To tackle this obstacle, some studies employ the quasi-3D method which applies two dimensional analysis of AFPM machines in the mean diameter [8], [9], [10]. Compared with the three dimensional Finite Element Method (3D-FEM), the results obtained from the quasi-3D are not sufficiently accurate. The only drawback of 3D-FEM is that it is time-consuming. This study

- *Narges Taran is graduated in masters degree program in Power Electronics and Electrical Machines in K. N. Toosi University of Technology, Iran. E-mail: nargess_taran@yahoo.com*
- *Dr. Mohammad Ardebili is currently head of Electrical Power Engineering Department of K. N. Toosi University of Technology, Tehran, Iran. Email: ardebili@eetd.kntu.ac.ir*

applies 3D-FEM as an assistant design tool simulation principle.

A 1 kW, 100 rpm AFPM generator consisting of 20 poles and 24 slots was designed and, using Genetic Algorithm (GA), its efficiency and power density were simultaneously improved to the optimized amounts.

2 Design of TORUS-S Generator

2.1 General Sizing Equations

Output power for any electrical machine can be expressed as [11]

$$P_{out} = \eta \frac{m}{T} \int_0^T e(t) i(t) dt = \eta m k_p E_{pk} I_{pk} \quad (1)$$

where m represents the number of phases and e(t) and E_{pk} stand for the phase air-gap EMF and its peak value. The currents i(t) and I_{pk} are the phase current and the peak phase current, and T is the period of one EMF cycle. The factor K_p signifies the electrical power waveform which equals 0.5cosφ for a sinusoidal design; cosφ is the power factor [12].

The EMF peak value in (1) for the axial flux machines is reached through

$$E_{pk} = k_e N_{ph} B_g \frac{f}{2p} (1 - \lambda^2) {D_o}^2 \quad (2)$$

where K_e is the EMF factor which incorporates the winding distribution factor (K_w) and the per unit portion of the total air gap area spanned by the salient poles of the machine (if any) [13], N_{ph} the number of turns per phase, B_g flux density in the air gap (also known as specific magnetic loading), f the frequency, p the number of poles, D_o the outer diameter of the machine, and λ is inner diameter to outer diameter ratio ($\lambda = D_i/D_o$) referred as diameter ratio while D_i represents the inner diameter of the machine.

The peak phase current in (1) is calculated as

$$I_{pk} = A \pi k_i \frac{1+\lambda}{2} \frac{D_o}{2 m_1 N_{ph}} \quad (3)$$

where m_1 indicates the number of phases in each stator and K_i is the current waveform factor whose value for the sinusoidal wave form is $\sqrt{2}$. The linear current density in the mean diameter known as the specific electrical loading could be calculated as follows:

$$A = \frac{m I_{rms} 2 N_{ph}}{\pi D_m} \quad (4)$$

where D_m presents the mean diameter ($D_m = \frac{D_i + D_o}{2}$).

Combining (1) through (3), the general purpose sizing equation takes the following form for AFPM:

$$P_{out} = \frac{m}{m_1} \frac{\pi}{2} k_e k_p k_i A B_g \eta \frac{f}{p} (1 - \lambda^2) \frac{1+\lambda}{2} {D_o}^3 \quad (5)$$

2.2 Sizing Equations for the TORUS-S

The generalized sizing equation approach can easily be applied to AFPM TORUS type generators [14].

From (5) the outer diameter can be calculated as

$$D_o = \left(\frac{P_{out}}{\frac{\pi}{2} k_e k_i k_p \eta B_g A \frac{f}{p} (1 - \lambda^2) \frac{1+\lambda}{2}} \right)^{\frac{1}{3}} \quad (6)$$

Inner diameter could be derived by the product of D_o and λ. The value of λ and its effect on the generator performance has been investigated by several articles. In practice, the optimal value for λ may differ depending upon the optimization goal. Moreover, given different electrical loading and flux densities, even when the optimization criterion remains unaltered, the optimal value for λ can vary according to the rated power, number of poles, frequency, etc. [15], [16], [17]. In the present study, the selection of the best value for λ was made by the optimization part.

The total axial length of the TORUS-S could be calculated by

$$L_{ax} = L_s + 2L_r + 2g \quad (7)$$

where L_{ax} stands for the total axial length, L_s and L_r are stator and rotor total thickness and g indicates one of the two airgap lengths. L_s can be expressed as

$$L_s = L_{cs} + 2d_{ss} \quad (8)$$

where L_{cs} is the stator core length and d_{ss} the stator slot depth. Equations (9) and (10) present them as

$$L_{cs} = \frac{B_g \pi \alpha_p D_o (1+\lambda)}{4 p B_{cs}} \quad (9)$$

$$d_{ss} = \frac{D_i - \sqrt{{D_i}^2 - \frac{2AD_m}{k_{cu} J_w}}}{2} \quad (10)$$

where α_p is the ratio of the pole-arc to pole-pitch, k_{cu} the slot fill factor and J_w the current density in the stator winding. Slot depth d_{ss} has been calculated in the mean diameter because the slots are parallel-sided. Accordingly, increasing the diameter leads to the widening of the tooth width, thus producing the smallest tooth width in the inner diameter. Thus, saturation starts from the inner diameter. In order to take the saturation hazard into account, the slot dimension calculations should be carried out in the inner diameter. B_{cs} is the stator core maximum flux density which, for the TORUS structure, can be estimated by (11) [17].

$$B_{cs} = \begin{cases} 5.47\, f^{-0.32} & f > 40\ Hz \\ 1.7\ to\ 1.8 & f \le 40\ Hz \end{cases} \quad (11)$$

The rotor axial length, L_r, becomes

$$L_r = L_{pm} + L_{cr} \quad (12)$$

L_{pm} is the magnet thickness, and L_{cr} which is the rotor core axial length can be expressed as

$$L_{cr} = \frac{B_g \pi D_o (1+\lambda)}{8 p B_{cr}} \quad (13)$$

B_{cr} is the rotor core maximum flux density and for the TORUS structure has been estimated to be between 1.6 T to 1.8 T [17].

2.3 Calculating the Efficiency

Machine efficiency can be expressed as

$$\eta = \frac{P_{out}}{P_{out} + P_{cu} + P_{Fe} + P_m} \quad (14)$$

where P_{cu}, P_{Fe} and P_m represent the copper, iron and mechan-

ical losses, respectively. Mechanical losses, being an insignificant fraction of total losses, were not taken into account [18]. The copper losses consist of ohmic and eddy current losses in wires as shown in (15).

$$P_{cu} = P_{RI^2} + P_{cu,eddy} \quad (15)$$

The ohmic loss was calculated using the phase resistance Rph and the phase current I_{ph} by (16).

$$P_{RI^2} = 3R_{phase}I^2 \quad (16)$$

Phase resistance can be calculated as follows

$$R_{ph} = \frac{\rho_{cu} L_{phase}}{a_{cu}} \quad (17)$$

where ρ_{cu} is the copper resistivity, a_{cu} the conductor cross section, and L_{phase} the conductor length per phase which, for a TORUS-S machine with coil pitch equal to one tooth (tooth concentrated winding configuration), can be calculated by

$$L_{phase} = N_{ph}(L + W_{ti} + W_{to}) + \pi D_o \quad (18)$$

Equation (18) is illustrated in Fig. 2. W_{ti} and W_{to} stand for the tooth width in the inner and outer diameter and L represents the effective length of each coil which could be calculated through outer and inner diameter subtraction.

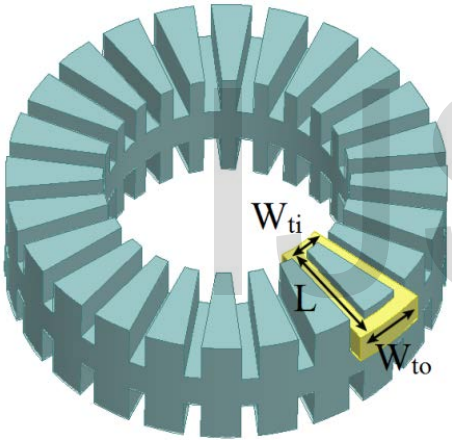

Fig. 2. The total length of a coil

Eddy current loss in winding can be calculated as

$$P_{cu,eddy} = K_{cu,eddy} f^2 {B_g}^2 \quad (19)$$

where $K_{cu,eddy}$ is dependent on wire material and its volume. Iron loss could be calculated by equation (20) which divides it into hysteresis, eddy current and an excess loss components:

$$P_{Fe} = k_h f {B_p}^{\alpha} + k_e f^2 {B_p}^2 + k_{exc} f^{1.5} {B_p}^{1.5} \quad (20)$$

In the above equation, B_p represents the peak flux density in the teeth. k_h, k_e and k_{exc} factors are dependent on the selected material and volume.

2.4 Calculating the Power Density

Upon calculating the main Dimensions, it becomes possible to calculate the power density through (21):

$$P_{density} = \frac{P_{out}}{\frac{\pi}{4} {D_t}^2 L_{ax}} \quad (21)$$

where D_t is the total outer diameter, encompassing the winding thickness.

3 Slot and Pole Number Combination

3.1 Choosing an optimal number of slots and poles to achieve a high winding factor

The number of stator slots and rotor poles should be selected properly to obtain suitable winding configuration. A good winding configuration must fulfill the following requirements:

- the winding factor has to be high enough so that the rated power of the generator is not reduced;
- it must make the best use of wires and avoid long end windings so that copper loss does not increase;
- it must reach the best copper utilization factor in the slots; and
- it must obtain a sinusoidal distribution of the MMF in order to avoid torque pulsations [19].

In low speed machines, eddy current losses are naturally small and there is no need to use complicated distributed winding which will result in unwanted copper losses. Overlapping and increasing coil pitch will lead to a longer length of inactive wire. Double-layer windings have a lower winding factor and copper fill factor. Therefore, a single-layer non-overlapped tooth concentrated winding (coil pitch equals one tooth) will be the simplest and most suitable configuration. It could be easily shown that the winding factor will be less than 0.866, which is not an ideal result, unless the value for the slot per pole per phase (q) falls between 0.25 and 0.5 [19], [20], [21]. As for the slot-pole number, a suitable combination should fulfill the following requirements:

- the number of slots should be an even number and a multiplier of the number of phases;
- the number of coils for each phase and the number of turns per coil should be an integer number;
- the Greatest Common Devisor (GCD) between the number of poles and slots indicates the number of times a winding configuration is repeated. Consequently, to obtain a balanced winding, the number of slots per phase should be divisible by GCD{ns,p}

When a DC output is required, the AC output of the generator is rectified so that no particular frequency of machine EMF is demanded. To have a frequency in the range of 15 to 25 Hz, with a generator speed of 100 rpm, the pole number should be in the range of 18 to 30. Table 1 represents acceptable combinations of slot-pole numbers and their corresponding fundamental winding factors. The bolded cells show the highest winding factor for each pole number candidate.

TABLE 1
Winding Factors for Different Slot-Pole Combination

p \ n_s	18	24	30	36	42
20	0.945	0.966	0.866		
22	0.902	0.958	0.874		
24	0.866			0.866	
26		0.958	0.936	0.870	
28		0.966	0.951	0.902	0.866
30				0.966	

3.2 Choosing an optimal number of slots and poles to achieve a low cogging torque

The next step is considering the impact of the slot-pole combination on the cogging torque. The cogging torque results from the magnetic force which attempts to maintain the alignment between the stator teeth and the permanent magnet poles. Therefore, the higher the number of poles and slots, the higher the cogging torque; and the higher the Least Common Multiple (LCM) between pole and slot numbers, the lower the cogging torque. The factor CT was introduced to denote the suitability of the slot-pole combinations in terms of the cogging torque [22]:

$$CT = \frac{pn_s}{LCM} \tag{22}$$

where p represents the number of poles, n_s the number of slots and LCM the Least Common Multiple between n_s and p. The larger the CT factor, the larger the cogging torque.

Table 2 presents different possible combinations for the number of poles and slots for a single-layer tooth concentrated winding with corresponding winding factors and CT factors. The selected combination contains 20 poles and 24 slots which leads to a high winding factor as well as a small CT.

TABLE 2
THE CT FACTOR FOR DIFFERENT POLE-SLOT COMBINATIONS

p	n_s	K_{w1}	LCM	CT
20	24	0.966	120	4
22	24	0.958	264	2
24	18	0.866	72	6
24	36	0.866	72	12
26	24	0.958	312	2
28	24	0.966	168	4
30	36	0.966	180	6

4 GENETIC ALGORITHM OPTIMIZATION

Due to the multiplicity of parameters involved in the design and the nonlinear equations complicating the relationship among the parameters, the problem at hand will not yield an optimized outcome through manual design, requiring soft computing methods. Genetic Algorithm (GA) is one of the most widely used population-based methods and stochastic search techniques. Its ability to search in vast, multi-dimensional spaces and its nonlinear nature make it indispensable to the optimization of electrical machines.

The optimization problem is expressed in terms of a set of parameters $X= \{x_1, x_2, \ldots, x_n\}$ where f(x), the objective function, can yield a maximum and minimum value. Utilizing simulated evolution, the solution space of the function is searched by the GA. In this case, X is referred to as a chromosome and $x_1, x_2, \ldots, x_n$ as genes. The combination of the three basic operators – that is, selection, crossover, and mutation – is used in the GA in order to simulate the evolution process. The fittest chromosomes in any population tend to reproduce and survive to the next generation, which helps improve subsequent generations [23]. The GA optimization method consists of the following steps:

i. Random generation of the initial population;
ii. Evaluation of the fitness of each chromosome;
iii. Termination condition or final generation (If YES, display superior chromosome. If NOT, go to next step);
iv. Reproduction of a new population using selection, mutation and crossover operators.
v. Back to step ii.

To use GA, it is necessary to specify a number of parameters as the genes constituting the chromosomes and to introduce objective functions into the algorithm via fitness function. In introducing the genes, it should be kept in mind that the parameters are not interconnected. The present study selected five parameters as genes: namely, specific magnetic loading, outer diameter, inner to outer diameter ratio, pole-pitch to pole-arc ratio and number of turns per phase. The parameters not selected as genes may be easily calculated through the equations mentioned above and the values assigned to the genes.

This study incorporates Genetic Algorithm to maximize both the efficiency and power density. The genes are chosen in a way that not only the parameters independent from one another but also the ones exerting the greatest influence on the objective function will be selected. Table 3 represents the generator characteristics and the selected genes as well as their restrictions in terms of efficiency and power density optimization.

TABLE 3
DESIGN REQUIREMENTS AND OPTIMIZATION RESTRICTIONS

Dimensional restrictions			
Outer diameter		D_o	$0.1 < D_o < o.8$
Inner to outer diameter ratio		λ	$0.4 < \lambda < 0.9$
Pole arc to pole pitch ratio		α_p	$0.6 < \alpha_p < 0.85$
Core and PM material limitations			
NdFeB PM	**Residual flux density**	B_r	1.1 [T]
	Relative permeability	μ_r	1.05 [H/m]
Maximum flux density in core		B_{cr}, B_{cs}	B_{cr}, $B_{cs} < 1.5$ [T]
Generator characteristics and restrictions			
Output power		P_{out}	1000 [W]
Rated speed		n	100 [rpm]
Rated voltage		V_{rms}	45 [v]
Output DC voltage		V_{DC}	110 [v]
Number of poles and slots		p/n_s	20/24
Magnetic loading		B_g	$0.4 < B_g < 1.2$
Number of turns per phase		N_{ph}	$80 < N_{ph} < 1500$

In order to execute the optimization algorithm, MATLAB's R2011a software optimization toolbox was used. Multi-objective GA is not very useful with regard to improving both of the selected objective functions via MATLAB's optimization toolbox. The reason is that the multi-objective optimization algorithm totalizes all objective functions attempting to increase the total sum of all objectives. Since the power density (expressed in W/cm^3) is smaller than the efficiency (expressed in percentage), the final result of the optimization, leading to higher improvement in the objective function with a lower value, improves the power density much more than the effi-

ciency. Fig. 3 shows the Pareto front achieved through the multi-objective method conducted in MATLAB's optimization toolbox. The horizontal axis represents efficiency in a way that moving to the left on the Pareto front curve increases the improvement on efficiency. The vertical axis represents power density in a way that moving to lower parts of the curve results in higher improvements on power density. As a result, the largest power density is obtained at point A which contains the lowest efficiency, and the highest efficiency is achieved at point B where power density is lowest. Table 4 represents the values for point A and B more clearly.

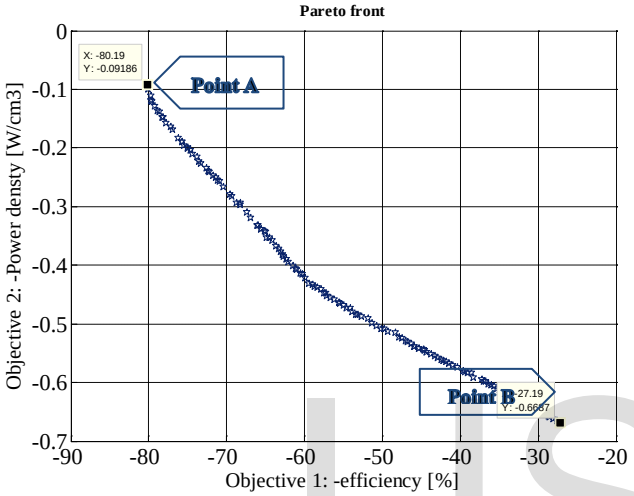

Fig. 3. Pareto Front for the multi-objective optimization

TABLE 4
VALUES FOR THE PARETO FRONT CRITICAL POINTS

Objective function	Efficiency [%]	Power density [W/cm3]
Point A	80.19	0.09
Point B	27.19	0.67

As Fig. 3 and Table 4 demonstrate, at point A the power density is very large but the efficiency is very low and thus unacceptable, while at point B the power density is high but the efficiency is still not sufficiently high. Therefore, the efficiency cannot be either of the suggested points obtained from the search space because neither is high enough. In other words, the multi-objective optimization is unable to optimize both objective functions, especially when their numerical values are from different levels with one of them being considerably smaller than the other. To tackle this obstacle, the following fitness function was introduced:

$$Fintness\ Function = a * \eta + b * P_{density} \qquad (23)$$

An increase in "a" leads to a greater emphasis on the efficiency so that the optimization process will improve the efficiency more than the power density while a rise in "b" leads to a greater emphasis on the power density so that the optimization process will improve the power density more than the efficiency. Nevertheless, the two parameters are not completely independent and the a/b ratio is significant. Fig. 4 displays the varying amounts of increase in the efficiency and power density corresponding to a/b ratios of 1 to 6. According to Fig. 4, one of the best compromises is achieved when a/b ratio equals 4.2. Therefore, a/b=4.2 was selected to execute the optimization algorithm. Of course, this selection is highly dependent on turbine necessities and the restrictions imposed on the suitable generator.

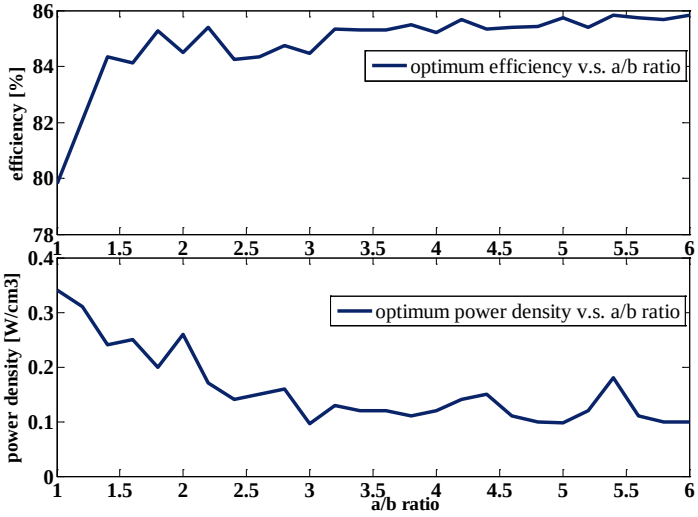

Fig. 4. Objective functions vs. a/b ratio

Since MATLAB's optimization toolbox only seeks out the minimum value, the fitness function was introduced to optimize the negative amount of (23). Fig. 5 shows that for a population of 400 for each generation, the fitness function converges after 500 generations. Table 5 presents the detailed specifications of the optimized slotted TORUS generator.

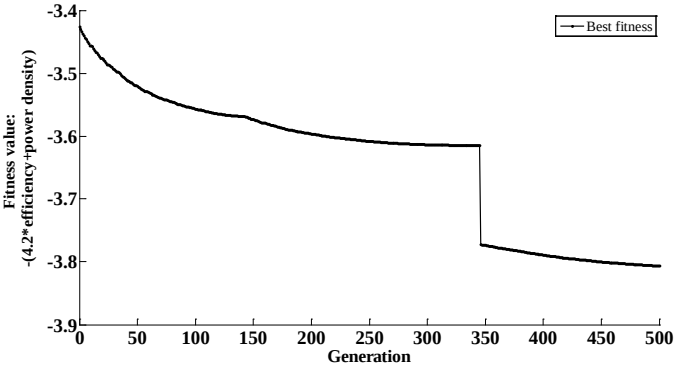

Fig. 5. Fitness function variation during GA optimization

TABLE 5
THE OPTIMIZED GENERATOR SPECIFICATIONS

Magnetic loading (B_g)	0.79 [T]	**Magnet thickness (L_{pm})**	4 [mm]
Outer diameter (D_o)	0.22 [m]	**Stator core axial length (L_{cs})**	10.3 [mm]
Pole arc/pole pitch (α_p)	0.65	**Rotor core axial length (L_{cr})**	11 [mm]
Inner/outer diameter (λ)	0.45	**Total axial length (L_{ax})**	120.5 [mm]
Number of turns/phase (N_{ph})	456	**Flux per pole per phase (ϕ_{pp})**	0.88 [mWb]
Specific electric loading (A)	25.3 [kA/m]	**EMF (E_{phase})**	25.28 [v]
Current density (J_w)	3.5 [A/mm^2]	**Resistance per phase (R_{phase})**	0.64 [Ω]
Slot width (w_s)	10 [mm]	**Synchronous reactance (X_{syn})**	12.23 [Wb]
Slot depth (d_{ss})	28 [mm]	**Power density**	0.14 [W/cm^3]
Airgap (g)	1 [mm]	**Efficiency (η)**	86.66 [%]

5 SIMULATION RESULTS

The performance of the generator was investigated using three dimensional finite element analysis and verified by Maxwell 14.0 3D simulation.

Figure 6 illustrates the flux density distribution and Fig. 7 its direction. It is evident that flux density is higher in close proximity to the PMs. The flux direction represents that opposite PMs are facing different poles (NS configuration for poles).

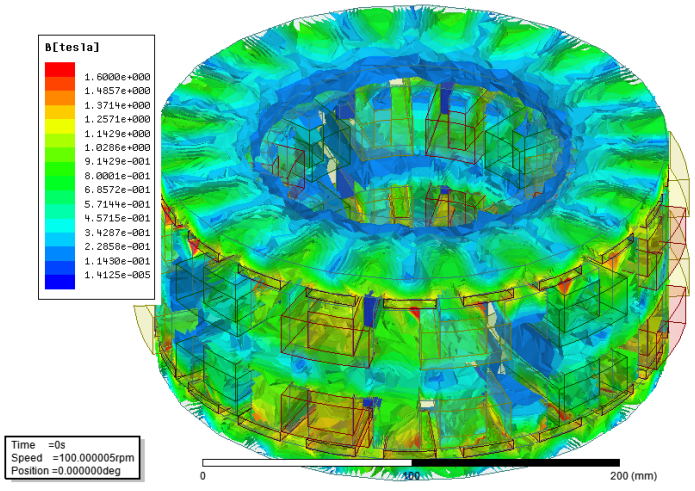

Fig. 6. Flux density distribution

Fig. 7. Flux directions

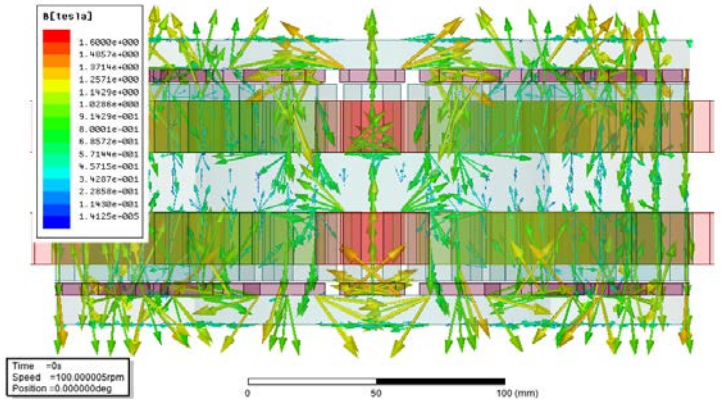

Core and teeth saturation adversely affects the operation of the machine because it reduces machine efficiency. To detect the saturation of either the core or the teeth, moreover, it is necessary to assess the magnetic flux density of the designed AFPM machine. Fig. 8 shows the air-gap flux density distribution with an average radius over two pole pairs. Fluctuations are due to inevitable phenomena such as the anisotropy of the rotor core and magnets. Also, the slotted stator increases distortions as well.

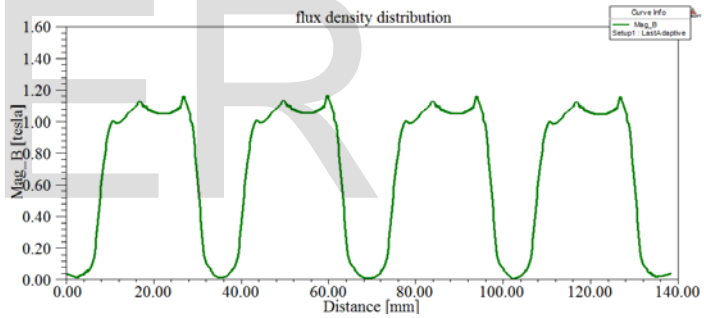

Fig. 8. Flux density in airgap over two pole pairs

The sinusoidal flux linkage obtained through a 180° rotation is depicted in Fig. 9.

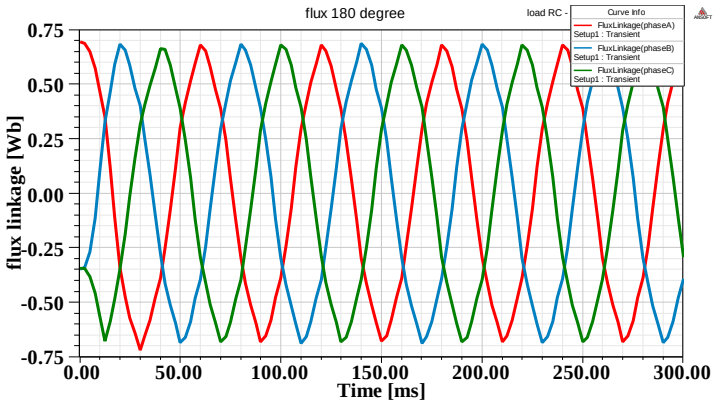

Fig. 9. Flux linkage waveforms

A three-phase bridge diode rectifier has been used to obtain the DC voltage. The load is a 100 ohm resistor placed in parallel to a low pass filter with the value of 220 µF in order to decrease the output DC voltage ripple. Fig. 10 presents bridge rectifier. The two stator side windings are connected in series and the star connection is used to avoid circulating currents. Obtained three-phase EMF whose rms amount is approximately 45v has been illustrated in Fig. 11.

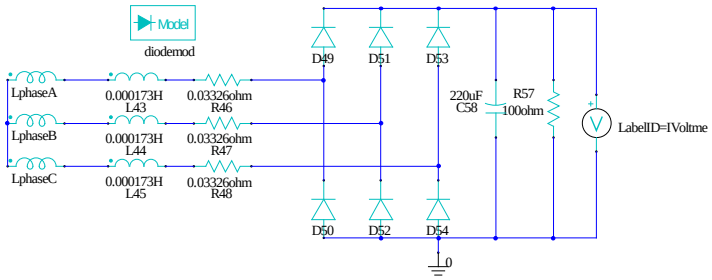

Fig. 10. Diode bridge rectifier

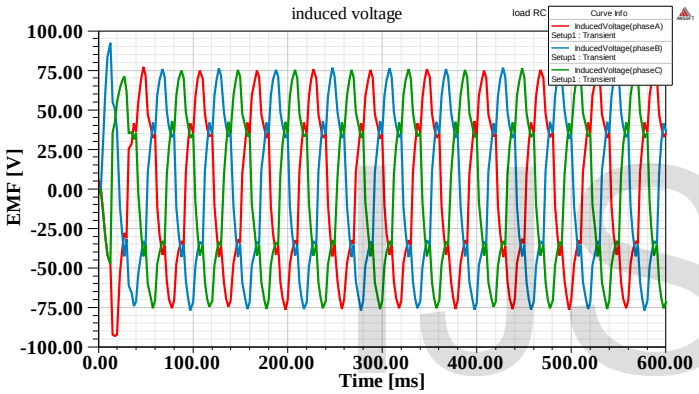

Fig. 11. The three-phase induced voltage (EMF)

According to (24) the resultant DC voltage should be about 110v.

$$V_{dc} = \sqrt{3}V_m = \sqrt{3}\sqrt{2}V_{rms} \quad (24)$$

where V_m is the maximum induced three-phase voltage.

The parallel capacitor works as a Low Pass Filter (LPF) in order to reduce the output DC voltage ripples. To illustrate this point, Fig. 12 represents the output DC voltage while there is no LPF and the ripple is about 15 v and Fig. 13 expresses the output DC voltage with a 220 µF capacitor paralleled with a 100 ohm load where the ripple has been reduced to one third, i.e. 5 v. Although by increasing the amount of the capacitor it is possible to decrease the DC voltage ripple, it will result in a high amount of current on diodes that could damage them. Fig. 14 depicts the three-phase current through a 180 degree rotation.

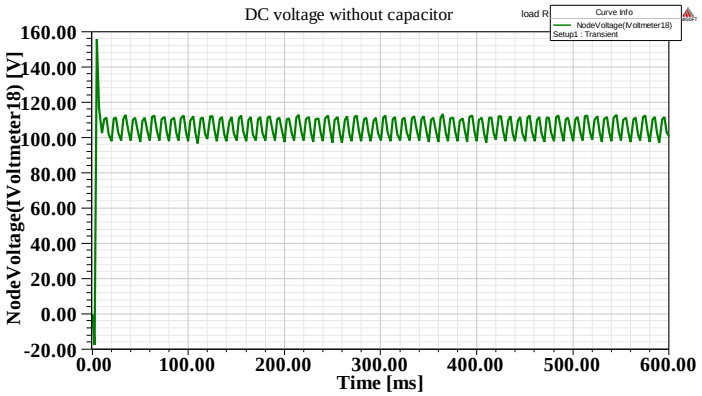

Fig. 12. Output DC voltage without LPF

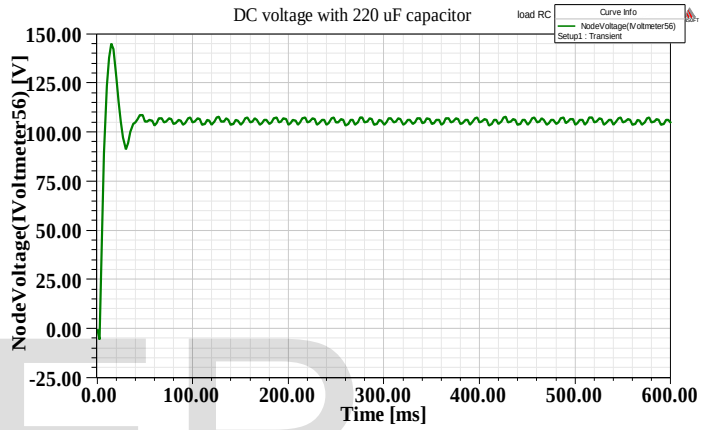

Fig. 13. Output DC voltage with LPF

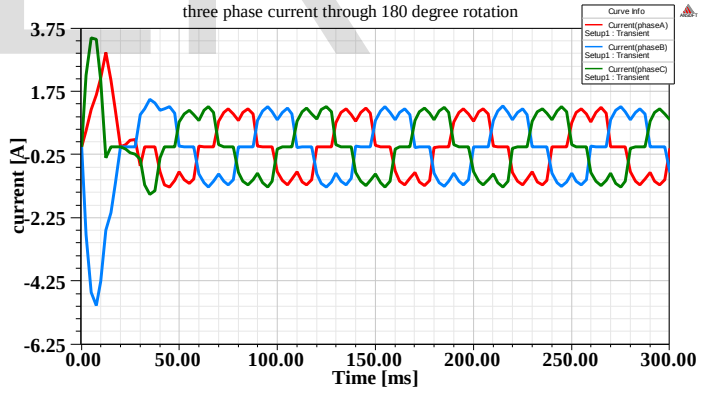

Fig. 14. Three-phase current waveform

6 Conclusion

The generator is the heart of any wind turbine and optimization may be said to be the most important part of its design and manufacture. Being fully compatible with wind turbine requirements, Axial Flux Permanent Magnet generators enjoy increasing popularity in the industry. In this paper, the design of a 1 kw, 100 rpm Axial Flux Permanent Magnet synchronous generator with TORUS-S structure for application in direct drive wind turbines is presented. A variety of slot-pole combinations were fully explored and the most suitable of them was selected (20 poles and 24 slots), leading to the lowest cogging torque and the highest efficiency. Single-objective optimizations

have already been the focus of a number of articles, but the simultaneous optimization of two essential parameters, efficiency and power density, has rarely been discussed. This paper offers a novel objective function via Genetic Algorithm to optimize the design of an AFPM generator with a TORUS-S topology. This objective function enables the optimization algorithm to favor efficiency over power density or vice versa. The ability to control the optimization focus allows the designer to achieve the optimum balance between the weight and size, on the one hand, and efficiency, on the other, depending on the location of the turbine and other similar factors which must be considered in the design. Therefore, the final result could be more suitable for this special purpose. Subsequently, the performance of the optimized generator was examined by finite element analysis three dimensional simulation. The results met the expected magnitudes which fully agree with the desired values.

Finally, it is worth mentioning that the design procedure and multi-objective optimization discussed in this paper is comprehensive and therefore easily applicable for similar design goals with different optimization objectives as well.

7 REFERENCES

[1] Soderlund, L., Koski, A., Vihriala, H., Eriksson, J-T., Perala, R., "Design of an Axial Flux Permanent Magnet Wind Power Generator", Eighth International Conference on Electrical Machines and Drives, (Conf. Publ. No. 444) , vol., no., pp.224,228, 1-3 Sep 1997.

[2] Chalmers, B.J., Wu, W., Spooner, E., "An Axial Flux Permanent Magnet Generator for a Gearless Wind Energy System", Proceedings of International Conference on Power Electronics, Drives and Energy Systems for Industrial Growth, , vol.1, no., pp.610, 8-11 Jan 1996.

[3] Wang, F., Pan, J., Zhang, Y., Cai, X., Liu, Y., Li, C., Du, J., "Design and Performance of Large Scale Direct-Driven Permanent Magnet Wind Generators", International Conference on Power Engineering, Energy and Electrical Drives (POWERENG), vol., no., pp.1,5, 11-13 May 2011.

[4] Spooner, E., Chalmers, BJ., "TORUS-Slotless, Toroidal-Stator, Permanent Magnet Generator", IEE proceedings-B electric power applications , Vol. 139, No.6, pp. 497-506, 1992.

[5] Eastham, J.F., Balchin, M. J., Betzer, T., Lai, H.C., Gair, S., "Disk Motor with Reduced Unsprung Mass for Direct EV Wheel Drive", IEEE Int. Symp. On Industrial Electronics, 1995.

[6] Profumo, F., Zhang, Z., Tenconi, A., "Axial Flux Machines Drives: A New Viable Solution for Electric Cars", IEEE Transactions on industrial electronics, Vol. 44, No.1, pp. 39-45, 1997.

[7] Zhang, Z., Profumo, F., Tenconi, A., "Axial Flux Wheel Machines for Electric Vehicles", IEEE Trans. on Electric Machines and Power Systems, 1996.

[8] Parvianien, A., Niemela, M., Pyrhonen, J., "Modelling of Axial Flux Permanent Magnet Machines", IEEE Transaction on industry applications, Vol. 40, No.5, pp. 1333-1340, 2004.

[9] Wibowo, H. A., Pradikta, A., Dahono, P.A., "An Analysis of Slotless Axial Flux Permanent Magnet Generators", Power Engineering and Renewable Energy (ICPERE), 2012 International Conference on , vol., no., pp.1,6, 3-5 July 2012.

[10] Ji-Young Lee, Dae-Hyun Koo, Seung-Ryul Moon, Choong-Kyu Han, "Design of an Axial Flux Permanent Magnet Generator for a Portable Hand Crank Generating System", IEEE Transactions on Magnetics, vol.48, no.11, pp.2977,2980, Nov. 2012.

[11] Huang, S., Luo, J., Leonardi, F., Lipo, T. A., "A General Approach to Sizing and Power Density Equations For Comparison Of Electrical Machines" , IEEE Trans. Ind. Appl., vol. 34, no. 1, pp. 92–97, Jan./Feb. 1998.

[12] Mahmoudi, A., Kahourzade, S., Rahim, N.A., Hew, W.P., "Design, Analysis, and Prototyping of an Axial Flux Permanent Magnet Motor Based on Genetic Algorithm and Finite Element Analysis", Magnetics, IEEE Transactions on , vol.49, no.4, pp.1479,1492, April 2013.

[13] Gholamian, A., Ardebili, M., Abbaszadeh, K., "Selecting of Slotted AFPM Motors with High Torque Density for Electric Vehicles", International Journal of Scientific & Engineering Research Volume 2, Issue 6, June 2011.

[14] Aydin, M., Huang, S., Lipo, T.A., "Design and 3D Electromagnetic Field Analysis of Non-Slotted and Slotted TORUS Type Axial Flux Surface Mounted Permanent Magnet Disc Machines", IEEE International Electric Machines and Drives Conference, IEMDC, vol., no., pp.645,651, 2001.

[15] Camplell, P., "Principle of a Performanent Magnet Axial Flux DC Machine", Proc.Inst. Elec.Eng,. vol. 121, No. 12, Dec. 1974.

[16] Jensen, C. C., Profumo, F., Lipo, T. A., " A Low Loss Permanent Magnet Brushless DC Motor Utilizing Tape Wound Amorphous Iron", IEEE Transactions On Industry Applications, vol. 28, No 3, pp 646-651, May/June. 1992.

[17] Huang, S., Luo, J., Leonardi, F., Lipo, T. A., "A Comparison of Power Density for Axial Flux Machines Based on the General Purpose Sizing Equation", IEEE Transactions on Energy Conv., vol. 14, Jan. 1999.

[18] Vansompel, H., Sergeant, P., Dupre, L., "Optimized Design Considering The Mass Influence of an Axial Flux Permanent Magnet Synchronous Generator with Concentrated Pole Windings", IEEE Transactions on Magnetics, vol.46, no.12, pp.4101,4107, Dec. 2010.

[19] Skaar, S. E., Krøvel, Ø., Nilssen, R., "Distribution, Coil-Span and Winding Factors for PM Machines with Concentrated Windings", Norwegian Research Council, Norway, 2006.

[20] Cistelecan, M.V., Popescu, M., Popescu, M., "Study of the Number of Slots/Pole Combinations for Low Speed Permanent Magnet Synchronous Generators", IEEE International Conference on Electric Machines & Drives Conference, 2007. IEMDC, May 2007.

[21] Florence Meier, "Permanent-Magnet Synchronous Machines with Non-Overlapping Concentrated Windings for Low-Speed Direct-Drive Applications", PhD thesis, Royal Institute of Technology, Stockholm, Sweden, 2008.

[22] Zhu, Z.Q., Howe, D., "Influence of Design Parameters on Cogging Torque in Permanent Magnet Machines", IEEE Transactions on Energy Conversion, , vol.15, no.4, pp.407,412, Dec 2000.

[23] Wrobel, R., Mellor, P.H., "Design Considerations of a Direct Drive Brushless Machine with Concentrated Windings", IEEE Transactions on Energy Conversion, vol.23, no.1, pp.1,8, March 2008.